International Journal of Heat and Mass Transfer 52 (2009) 4308–4316

Contents lists available at ScienceDirect

International Journal of Heat and Mass Transfer

journal homepage: www.elsevier.com/locate/ijhmt

The influence of rotational charge motion intensity on nitric oxide formation in gas-engine cylinder

R.Z. Kavtaradze, D.O. Onishchenko, A.A. Zelentsov *, S.S. Sergeev

Bauman Moscow State Technical University, 2-nd Baumanskaya, 5, Moscow 105005, Russia

ARTICLE INFO

Article history:
Received 7 October 2008
Received in revised form 27 February 2009
Accepted 31 March 2009
Available online 21 May 2009

Keywords:
Gas engine
Natural gas
Heat transfer
Nitric oxide
Rotational charge motion intensity

ABSTRACT

There has been studied the influence of rotational number on the modification of local thermophysical features of working medium in the process of diesel combustion, converted into natural gas with spark ignition. Mathematic model, which is three-dimensional transient Reynold's equations with addition of k–ε turbulence model, is realized with the help of software complex FIRE. We analyze the results of numerical experiments, give the figures of transient local and average in volume features of working medium, such as turbulent kinetic energy, velocity, temperature. Local nitric oxide formation in the process of combustion is determined on the basis of Zeldovich's expanded thermal mechanism. Comparative analysis of numerical research results at the design stage allows us to get optimal level of rotational charge motion intensity and ignition point, which improve ecological characteristics of the diesel at its conversion into gas engine with spark ignition.

1. Introduction

Energy and ecological situation in the world on the whole points to the fact that natural gas the main component of which is methane finds its use as an engine fuel and is considered as an alternative to fluid carbon fuels nowadays. In this article, we are studying the process of serial diesel KamAZ (number of cylinders is eight, bore size and piston stroke are equal 120 mm) conversion into the gas engine with spark ignition which works on natural gas. There are several demands to follow which it is necessary to convert diesel into the gas engine:

1. Decrease of gas-engine compression in comparison with basic engine in order to eliminate detonation; it was done by means of volume increase (reboring) of serial chamber which is in the piston.
2. Provision of inner carburetion by means of natural gas injection into inlet system and its intensive mixing with air.
3. Forced ignition (by means of electric spark) of gas–air compound in the cylinder at the end of compression process.

It is known that optimal charge spin in serial diesel cylinder, which starts when fuel intakes and goes on up to the moment of its injection and firing, makes for quality improvement of carburetion and firing processes. This fact, in its turn, influences both the toxic agent emission and the efficacy of engine work [1]. This question has not been studied yet for gas engines [2]. The article shows that optimal combinations of rotational charge motion intensity and sparking point of fuel makes for essential decrease of nitric oxides concentration in the products of gas-engine combustion.

2. Modeling of non-stationary transport and turbulent combustion processes in the engine cylinder

The differential equations in private derivatives with the help of which physical processes of transfer of quantity movement are described, energy, weights and concentration can be written down in the form of the generalised law of the preservation expressed by the differential equation in the form of balance of non-stationary and convectional, on the one hand, and diffusion and source currents, on the other hand [3,4]:

$$\frac{\partial}{\partial\tau}(\rho\Phi) + div\left(\rho\vec{W}\Phi\right) = div(\Gamma_\Phi grad\Phi) + S_\Phi, \quad (1)$$

where ρ, density; W, velocity; Φ, undefined dependent variable; Γ_Φ, diffusion factor; S_Φ, source member which in general it is possible to present as a difference of generation S_{Φ_g} and annihilation $S_{\Phi a}$ of heat flux, i.e. $S_\Phi = S_{\Phi_g} - S_{\Phi a}$. The concrete kind Γ_Φ and S_Φ, together S_{Φ_g} with $S_{\Phi a}$ depends on variable meaning (Table 1). In Table 1, tensor form of record of the Eq. (1) for the Cartesian system of coordinates is given, besides, in other equations from Table 1 the following designations are accepted: p, pressure, G_i, volume force; $V_\mu = \frac{1}{3}\mu \cdot grad\left(div\vec{W}\right)$, a member expressing volume deformation;

* Corresponding author. Tel.: +7 499 265 78 92.
E-mail addresses: kavtar@power.bmstu.ru (R.Z. Kavtaradze), zelentsov.aa@gmail.com (A.A. Zelentsov).

0017-9310/$ - see front matter © 2009 Elsevier Ltd. All rights reserved.
doi:10.1016/j.ijheatmasstransfer.2009.03.060

Nomenclature

C	concentration (kg m^{-3})
D	diffusion factor
G_i	volume force (N m^{-3})
k	turbulence kinetic energy (m^2 s^2)
L_0	mass stoichiometric air quantity
$\dot{m}$	mass flux (kg m^{-3} s^{-1})
$M_{\max}$	maximum value of engine torque (N m)
n	crankshaft frequency (min^{-1})
N_e	effective power (kW)
p	pressure (bar)
p_z	maximum value of pressure (bar)
P	kinetic energy generation of turbulence at the expense of flux deformation = $-\overline{W_i'W_j'}\frac{\partial W_i}{\partial x_j}$
Pr	Prandtl number
q_v	heat intensity source (Wm m^{-3})
Q_r	quantity of heat allocated as a result of chemical reaction per a mass unit (J kg^{-1})
Re	Reynolds number
S_{ij}	mean rate of strain = $\frac{1}{2}\left(\frac{\partial W_i}{\partial x_j}+\frac{\partial W_j}{\partial x_i}\right)$
S_Φ	source member
S_{Φ_g}	generation of dependent variable
$S_{\Phi a}$	annihilation of dependent variable
t	averaging period (s)
T	temperature (K)
T_z	maximum value of temperature (K)
u^+	dimensionless coordinate of "wall laws"
W_i	velocity (m s^{-1})
y^+	dimensionless coordinate of "wall laws"

Greek symbols

δ_{ij}	Kroneker symbol
Γ_Φ	diffusion factor
ε	dissipation rate of turbulence kinetic energy (m^2 s^{-3})
Φ	undefined dependent variable
$\overline{\Phi}$	mean value of dependent variable
Φ'	fluctuations around the mean value of dependent variable
λ	excess-air ratio; thermal conductivity (W m^{-1} K^{-1})
μ	dynamic viscosity (N s m^{-2})
μ_T	eddy (turbulent) viscosity (N s m^{-2})
∇q_R	radiating heat flux from a radiation source = $\frac{\partial q_R}{\partial x_j}$ (W m^{-3})
ρ	density (kg m^{-3})
τ	time (s)

μ, dynamic viscosity; λ, heat conductivity; δ_{ij}, Kroneker symbol; D, diffusion factor; $\dot{m}$, intensity of weight source of weight (speed of weight change of chemical components in volume unit). The radiating heat flux from a radiation source $\nabla q_R = \frac{\partial q_R}{\partial x_j}$ plays an essential role only in the course of heterogeneous combustion of the liquid diesel fuel accompanying with occurrence of microparticles of soot – the basic generators of radiation. Thus, radiation of gaseous products of combustion is very small [3,4]. In this connection in case of gas-engines heat flux from a radiation source can be considered.

Using Reynolds' approach according to which instant value of any parameter Φ is represented as its sum averaged in time and pulsating Φ values, i.e. $\Phi = \overline{\Phi} + \Phi'$ where $\overline{\Phi} = \frac{1}{t}\int_{\tau_0}^{\tau_0+t}\Phi(\tau)d\tau$ it is the averaging period, initial system of transport equation is replaced with open-loop system of the equations in the form of Reynolds (see Table 1) for closing of which k–ε turbulence model is used. The standard form of this model used for the description of turbulent transport processes in engine cylinder looks like [5–7]:

$$\rho\frac{\partial\bar{k}}{\partial\tau}+\rho W_j\frac{\partial\bar{k}}{\partial x_j}=P+G-\bar{\varepsilon}+\frac{\partial}{\partial x_j}\left(\mu+\frac{\mu_T}{\mathrm{Pr}_{TDk}}\frac{\partial\bar{k}}{\partial x_j}\right);$$
$$\rho\frac{D\bar{\varepsilon}}{D\tau}=\left(C_{\varepsilon1}P+C_{\varepsilon3}G+C_{\varepsilon4}\bar{k}\frac{\partial W_k}{\partial x_k}-C_{\varepsilon2}\bar{\varepsilon}\right)\frac{\bar{\varepsilon}}{\bar{k}}+\frac{\partial}{\partial x_j}\left(\frac{\mu_T}{\mathrm{Pr}_{T_\varepsilon}}\frac{\partial\bar{\varepsilon}}{\partial x_j}\right), \qquad (2)$$

Table 1
The equations of conservation laws, as special cases of the generalised differential equation (1).

The generalised differential equation (vector and tensor form): $\frac{\partial}{\partial\tau}(\rho\Phi)+div\left(\rho\vec{W}\Phi\right)=div(\Gamma_\Phi grad\Phi)+S_\Phi \iff \frac{\partial}{\partial\tau}(\rho\Phi)+\frac{\partial}{\partial x_j}(\rho W_j\Phi)=\frac{\partial}{\partial x_j}\left(\Gamma_\Phi\frac{\partial\Phi}{\partial x_j}\right)+S_\Phi$

$\Phi=W_i,\Gamma_\Phi=\mu$	The initial form	$\rho\frac{DW_i}{D\tau}=G_i-\frac{\partial p}{\partial x_i}+\frac{\partial}{\partial x_j}\left[\mu\left(\frac{\partial W_i}{\partial x_j}+\frac{\partial W_j}{\partial x_i}-\frac{2}{3}\delta_{ij}\frac{\partial W_k}{\partial x_k}\right)\right]$ $i,j,k=1,2,3$
$S_\Phi=G_i-\frac{\partial p}{\partial x_i}+V_\mu$	Reynolds's form	$\bar{\rho}\frac{D\overline{W_i}}{D\tau}=\overline{G_i}-\frac{\partial p}{\partial x_i}+\frac{\partial}{\partial x_j}\left[\mu\left(\frac{\partial\overline{W_i}}{\partial x_j}+\frac{\partial\overline{W_j}}{\partial x_i}-\frac{2}{3}\delta_{ij}\frac{\partial\overline{W_k}}{\partial x_k}\right)-\bar{\rho}\overline{W_i'W_j'}\right]$
Movement quantity conservation equation (Nave–Stocks equation)	New unknowns	where $\bar{\rho}\overline{W_i'W_j'}$ – Reynold's tensor of turbulent tension, defined on pulsating velocity components $\overline{\tau_{ij}}=\mu\left(\frac{\partial\overline{W_i}}{\partial x_j}+\frac{\partial\overline{W_j}}{\partial x_i}-\frac{2}{3}\delta_{ij}\frac{\partial\overline{W_k}}{\partial x_k}\right)$ – viscous (turbulent) tension tensor, defined on averaged values of speed components
$\Phi=h,\Gamma_\Phi=\frac{\lambda}{c_p}$,	The initial form	$\rho\frac{\partial H}{\partial\tau}+\rho W_j\frac{\partial H}{\partial x_j}=\frac{\partial}{\partial x_j}\left(\lambda\frac{\partial T}{\partial x_j}\right)+\frac{\partial p}{\partial\tau}+\frac{\partial}{\partial x_i}(\tau_{ij}W_j)+\rho G_jW_j-w_rQ_r-\nabla q_R$
$S_\Phi=\frac{\partial p}{\partial\tau}+\frac{\partial}{\partial x_i}(\tau_{ij}W_j)+\rho G_jW_j-w_rQ_r-\nabla q_R$	Reynolds's form	$\bar{\rho}\frac{\partial\overline{H}}{\partial\tau}+\bar{\rho}\overline{W_j}\frac{\partial\overline{H}}{\partial x_j}=\frac{\partial}{\partial x_j}\left(\lambda\frac{\partial\overline{T}}{\partial x_j}-c_p\bar{\rho}\overline{T'W_j'}\right)+\frac{\partial\bar{p}}{\partial\tau}+\frac{\partial}{\partial x_i}(\overline{\tau_{ij}}\overline{W_j})+\bar{\rho}\overline{G_jW_j}-\overline{w_rQ_r}-\nabla\bar{q}_R$
Energy conservation equation	New unknowns	where $c_p\bar{\rho}\overline{T'W_j'}$ – turbulent transport of enthalpy; $\bar{\rho}c_pT'$ by means of speed fluctuation W_j'
$\Phi=1,\Gamma_\Phi=0,S_\Phi=0$	The initial form	$\frac{\partial\rho}{\partial\tau}+\frac{\partial}{\partial x_i}(\rho W_i)=0$
Mass conservation equation (continuity equation)	Reynolds's form	$\frac{\partial\bar{\rho}}{\partial\tau}+\frac{\partial}{\partial x_j}(\bar{\rho}\cdot\overline{W_j})=0$
$\Phi=\frac{C_i}{\rho},\Gamma_\Phi=D_i\rho$	The initial form	$\frac{DC}{D\tau}=\frac{\partial C}{\partial\tau}+W_j\frac{\partial C}{\partial x_j}=\frac{\partial}{\partial x_j}\left(D\frac{\partial C}{\partial x_j}\right)+\dot{m}$ $(i,j,k=1,2,3)$
$S_\Phi=\dot{m}_l$	Reynolds's form	$\frac{D\overline{C}}{D\tau}=\frac{\partial\overline{C}}{\partial\tau}+\overline{W}_j\frac{\partial\overline{C}}{\partial x_j}=\frac{\partial}{\partial x_j}\left(D\frac{\partial\overline{C}}{\partial x_j}-\bar{\rho}\overline{C'W_j'}\right)+\dot{m}$
Diffusion (concentration) equation	New unknowns	where $\bar{\rho}\overline{C'W_j'}$ turbulent diffusion transport of component mass with concentration C by means of speed fluctuation W_j'

Table 2
Values of empirical factors of k–ε turbulence model.

C_μ	$C_{\varepsilon 1}$	$C_{\varepsilon 2}$	$C_{\varepsilon 3}$	$C_{\varepsilon 4}$	Pr_{TDk}	$\mathrm{Pr}_{T\varepsilon}$	Pr_T
0.09	1.44	1.92	0.8	0.33	1	1.3	0.9

Distributions velocity and temperature distribution in a turbulent interface is set in dimensionless coordinates of "wall laws" (y^+, u^+).

where composed $P = -\overline{W_i' W_j'}\frac{\partial W_i}{\partial x_j} = 2\nu_T S_{ij} S_{ij} - \frac{2}{3}(\mu_T S_{kk} + \bar{k})S_{kk}, G = -g_i \frac{\mu_T}{\mathrm{Pr}_T}\frac{\partial \rho}{\partial x_i}$ point out at turbulence kinetic energy generation at the expense of deformation of the flux and at the expense of volume forces accordingly. Thus, $S_{ij} = \frac{1}{2}\left(\frac{\partial W_i}{\partial x_j} + \frac{\partial W_j}{\partial x_i}\right), \mu_T = C_\mu \bar{\rho}\frac{\bar{k}^2}{\bar{\varepsilon}}$.

Empirical factors and experimental values of Prandtl turbulent number for model used are given in Table 2.

Turbulence equations of k–ε models (2) for Reynolds's $\mathrm{Re} = \frac{\sqrt{k}\cdot l}{\nu}$ high numbers are applied to the areas remote enough from walls of a combustion chamber in which influence of molecular viscosity is very small in comparison with turbulent viscosity, and damping wall influence can be neglected.

It is necessary to note Spalding's and its school merit in the development of turbulence theory [5,6] and in combustion theory [8]. The results, he received, have found embodiments in the universal software package PHOENICS, which is used to calculate combustion processes. In the present work for modeling of a flow with Reynolds's low number, occurring in a turbulent interface, it is necessary to set boundary conditions for k in control volumes adjoining a combustion chamber wall. This task is carried out with the help "wall-boundary functions", offered by Launder and Spalding [5,6], representing a set of semi-empirical functions obtained on the basis of experimental researches and the theory of similarity.

3. Modeling of nitric oxides formation in combustion processes

Close interaction between various physical processes (weight, quantity of movement and energy transport) and the chemical reactions of combustion simultaneously occurring in cylinder volume is characteristic for working process of piston engines.

Heat generation at combustion causes pressure, temperatures and density gradients and, of course, contributes into transport processes. In transport equations the influence of chemical process of combustion is considered by presence of the so-called "source" members such, as a source of heat intensity $q_v = [\mathrm{W/m^3}]$ and a source of mass intensity $\dot{m} = [\mathrm{kg/(m^3\ s)}]$ (see Table 1). These parameters values can be calculated by means of speed of chemical reaction of combustion W_r:

$$q_v = Q_r W_r; \quad \dot{m} = -W_r, \tag{3}$$

where $Q_r = [\mathrm{J/kg}]$ is the quantity of heat allocated as a result of chemical reaction per a mass unit. Speed of chemical reaction of combustion is defined on the basis of combustion model offered by Magnussen and Hjertager [9]. According to this model the gas mixture consists, generally, of fuel, oxygen, products of combustion and inert gases (nitrogen), at the same time, these fractions masses, accordingly, should be calculated. The model is based on a hypothesis according to which in a turbulent flame reagents (fuel and oxygen) contain in the same whirlwinds and are separated from whirlwinds in which there are hot products of combustion. Chemical reactions usually have a time scale, which is very short in comparison with a characteristic time scale of turbulent process of transport. It allows to assume that chemical reactions in small turbulent structures (in whirlwinds) go almost instantly before their ending as soon as there is a mixing of reagents at molecular level. In this connection it is accepted that combustion speed is defined by mixing speed in the whirlwinds containing reagents, and that, containing combustion materials, i.e. dissipation speed of these whirlwinds defines the speed of combustion. Local kinetic energy of turbulence is represented as a defining parameter for reagents mixing speed [11]. The peculiarity of the model is that it does not demand the fluctuation setting of mass fraction of fuel, oxygen, combustion materials and inert gases (nitrogen) – $m_T, m_{O_2}, m_{np.cz.}$ and m_{in}. As a result an average speed of reaction of fuel combustion is registered as follows [10]:

$$\overline{w_r}_{MH} = \frac{B}{\tau_t}\bar{\rho}\min\left(\bar{m}_T, \frac{\bar{m}_{O_2}}{L_0}, C\frac{\bar{m}_{np.cz}}{1+L_0}\right), \tag{4}$$

where L_0, mass stoichiometric air quantity; $\tau_t = \frac{\bar{k}}{\bar{\varepsilon}}$, a time scale of turbulent mixing; B and C, the empirical factors, considering influence of turbulence and fuel parameters on chemical reaction speed.

In combustion materials of the piston engine the quantity of NO makes more than 90% from total quantity of all nitric oxides NO_x and consequently in calculations the model of NO formation is used, as a rule. Nitric oxide is formed in a combustion chamber in zones with high temperatures ($T > 1800$ K), and further, at long stay under atmospheric conditions it almost completely turns into nitrogen dioxide NO_2 [10]. There are three schemes of nitric oxide origin in a combustion process: fuel NO which is formed of the fuel nitrogen; "fast" NO (Prompt – NO) which is formed already in the front of the flame from the nitrogen, being in the air according to S Fenimore's mechanism; and thermal NO which is formed in high-temperature combustion materials from the nitrogen being in the air according to Zeldovich's mechanism. It is known that in piston engines ~5–10% from total nitric oxides are formed on Fenimore's mechanism ("fast" NO) and ~90–95% on Zeldovich's mechanism (thermal NO) [2,10]. Transformation of the nitrogen containing in fuel, into nitric oxide in a combustion process in piston engines practically does not play any role as fuel for these engines almost does not contain any fixed nitrogen. Reasoning from it, in the given work the thermal mechanism of NO formation from atmospheric nitrogen (the so-called expanded Zeldovich's mechanism) according to which nitrogen oxidation occurs as a chain mechanism, the basic reactions of which are:

$$\mathrm{O + N_2 \leftrightarrow NO + N}; \quad \mathrm{N + O_2 \leftrightarrow NO + O}; \quad \mathrm{N + OH \leftrightarrow NO + H}. \tag{5}$$

Thus, the speed of NO formation depends on the maximum combustion temperature, concentration of oxygen and nitrogen in products of combustion and does not depend on the chemical nature of fuel. The results received on the basis of the expanded Zeldovich's mechanism (5), as a rule, correspond to experimental data [12]. It is obvious that intensive NO formation occurs in local volume zones of the combustion chamber with high temperatures, where local values of excess coefficient is $\lambda \approx 1$ [12–14].

4. Numerical integration of transport equations

Method SIMPLE (semi-implicit method for pressure-linked equations) for numerical integration of transport equations is used. It is a semi-implicit method for the equations connecting pressure. This method was developed by Patankar and Spalding [15,16] and is used for calculation of subsonic flows. The method means calculations on stages like "predictor–corrector".

In the beginning preliminary pressure values p^0 and speed component are defined u^0, v^0, w^0 (i.e. speed vector), and then correcting amendments p' and u', v', w' (i.e. W') is calculated in such a way that true parameters values are presented as

$$p = p^0 + p'; \quad u = u^0 + u', \quad v = v^0 + v', \quad w = w^0 + w',$$
$$\vec{W} = \vec{W^0} + \vec{W'}. \tag{6}$$

Amendments to pressure are connected with amendments to speed components approached to movement equations leading to

Puasson's equation which is solved concerning the amendment to pressure p'. Let us notice that if the calculated speed vector W^0 satisfies to the continuity equation in each point amendments to pressure p' will be equal to zero in each point. Algorithm SIMPLE and calculation procedure are in detail stated in Refs. [5,15,16].

For numerical integration of equation system in the Reynolds-averaged form (see Table 1) together with k–ε models equations (2), and also with chemical kinetic equations, in the present work it is used AVL FIRE – software product 3D-CFD [15], focused on and adapted to the solution of specific piston engines problems and thereby having an advantage in comparison with the well-known multiple-purpose programs FLUENT, ANSYS/Flotran, Star CD, etc. [15,17]. Besides, FIRE allows to use mobile grids and thereby to provide the presence of moving details (piston, valve).

Four variants of experimental chambers in piston were preliminary investigated: symmetric, displaced, conical, ω – figurative. As these researches have shown, from all investigated experimental chambers, the symmetric (cylindrical) form of a combustion chamber located in piston, is more suitable, from the point of its ecological status, and efficacy (see Table 3). Fig. 1 shows the developed design of the combustion chamber mounted on the experimental gas engine, and also its breakdown into control volumes.

Division of computational grid area into control volumes is carried out by means of the special program Mesh Generator, including on program complex FIRE [15]. It is necessary to underline that successfully constructed computational grid is an important step to the successful result, comparable in value with a choice of turbulence model. The special attention at computational grid construction is given to characteristic places in the engine cylinder, such as areas of an spark plug location, or combustion chamber edges in the piston. For chambers investigated there have been generated grids with the average cell size of 5 mm. For characteristic areas this size reached 0.5 mm. Total number of control volumes was about 80,000 cells, thus the computational area consists on ~80% from cells of hexagonal and on ~20% from cells of tetrahedral forms. At piston moving to the top dead point (TDP), cells of a computational grid are being compressed along a cylinder axis, and at piston movement to the bottom dead point (BDP) they are stretched.

5. Short description of experimental installation. Mathematical model verification

The experimental gas engine works with the distributed natural gas injection and with a turbo-supercharging. In it, as well as in a base diesel engine, the combustion chamber as it was already marked, – semi-divided, however chambers of serial and experimental engines differs in their sizes essentially (see Fig. 1, and also Table 3). At diesel engine converting, the spark plug has been placed instead of a fuel injection nozzle. Gas fuel injection valves of inlet channels are mounted. There is one inlet and one outlet valves on each cylinder. The inlet channel of tangential type provides an intensive rotation of gas–air charge at inlet. Combustion chamber volume in the cylinder is increased by completion of a fire piston head. It has led to a compression ratio reduction with 17 to 11.25–11.27 that has accordingly affected the capacity of the experimental engine (see Table 3).

For an experimental research of the working process of the diesel engine converted into the gas engine in VNIIGAZ laboratory the special stand has been created the scheme of which is given in Fig. 2. The program of experimental researches, except measurements of characteristic parameters, such as effective values of a rotational moment, capacity, the fuel expense consumption, etc., also provided engine indication, and also concentration measurement of nitric oxides in exhausts on various high-speed and loading power setting.

Engine start-up is realized by a command from a control panel 1 after which the unloading device 2 starts an engine 3 crankshaft rotation. The signal from the gauge of a crankshaft position 4 at first is received by multiplier 13, and then by receiver 10 where there is its processing and synchronisation with a signal of the high pressure gauge 8 located in the engine cylinder. The signal arrives at first at the booster 12, and then is processed by the processor 10. The cooling system of the high pressure gauge 8 is a closed-loop system, volume of a cooling tank 9 makes 20 L. Adjustment of a throttle position, change of a loading size is conducted from a control panel 1. The signal with lambda-gauge 5 was processed by means of gas analyzer STARGAS 898 of infra-red action type 11, through which measurements of toxic substances concentration in the exhausts and of air excess factor were carried out. Natural gas consumption was defined by calculation, using the measured values of pressure and gas temperatures in the channel after a high pressure reducer 6. Rotational moment and capacity measurement was carried out under the known scheme.

Piezo-quartz high pressure gauge 8QP505 manufacture by AVL (Austria) has been used to read the display diagram of the engine. The gauge has the following characteristics: measurement range 180 bar; sensitivity 18.65 mV/bar; linearity $< \pm 0.6\%$; own frequency 100 kHz. The basic device – Digital Analyzer 657 AVL – the device of reception and processing of signals consists of the booster 12, the processor 10 and the display. Registration of non-stationary pressure in the engine cylinder is carried out as follows: the signal (mV) from the high pressure gauge 8QP505 8 arrives at the booster block 12, then in the processor 10 where there is its synchronization and processing to the signal which has arrived from the measuring device 4 of the crankshaft speed. The device 4 consists of a plastic disk 4 with initialization and the optical gauge.

Verification of the mathematical model of turbulent transport and combustion in the gas-engine cylinder is realized by

Table 3
Technical characteristics of a serial diesel engine of KamAz-740.13-240 and its experimental version converted into a gas engine.

Engine model	Serial diesel engine of KamAz-740.13-240	The experimental version converted into a gas engine
Engine type	Diesel engine with direct injection and with a turbo-supercharging	Gas internal-combustion engine with a spark ignition and a turbo-supercharging
Fuel	Diesel fuel	Natural gas ($\sim 95\%$ CH_4)
N_e, [kW], at n, [min^{-1}]	191 at 2200	176 at 2200
M_{rmax} [N m] at n, [min^{-1}]	931 at 1300–1500	864 at 1300–1500
Cylinder diameter/piston stroke, D/S, [mm/mm]	120/120	120/120
Compression degree, ε, [–]	17	11.25–11.27
Number and arrangement of cylinders	8, V-form	8, V-form
Combustion chamber type	Semi-divided, the chamber in the piston (symmetric)	Semi-divided, the chamber in the piston (four variants of experimental chambers: symmetric, shifted, conical, ω-shaped)

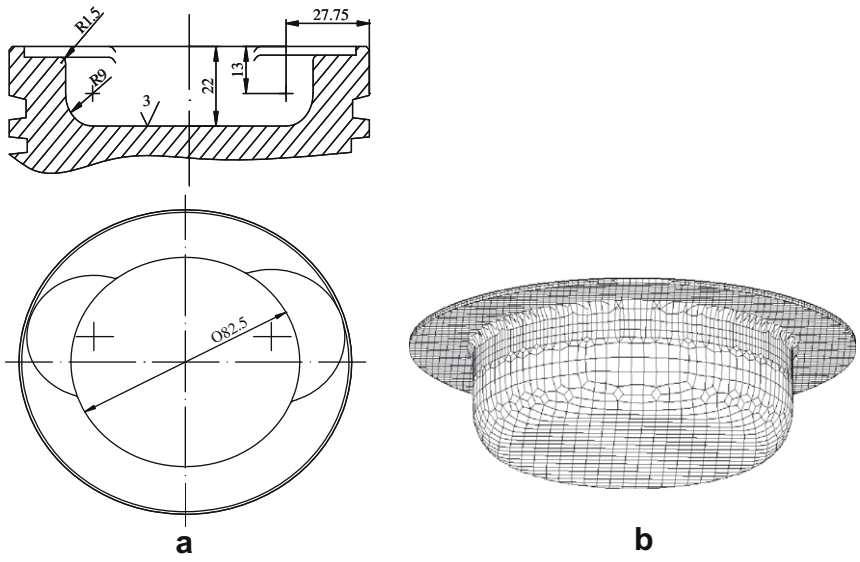

Fig. 1. Design of combustion chamber located in the piston of an experimental gas engine (a), and its representation in the form of control volumes (b).

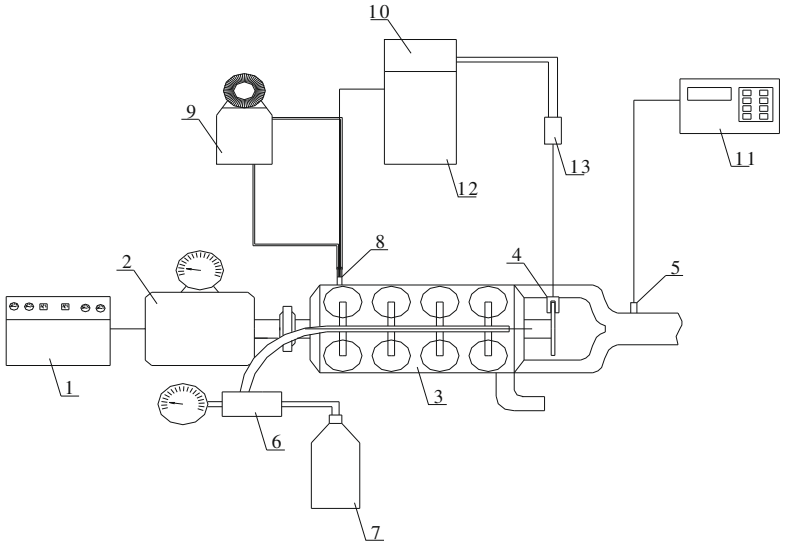

Fig. 2. The schematic experimental installation: 1, control board; 2, unloading device; 3, engine; 4, gauge for crankshaft position registration; 5, a lambda-gauge; 6, high pressure reducer; 7, gas bag; 8, high pressure gauge; 9, cooling device of high pressure gauge; 10, device of reception and processing of a signal from gauges 4 and 8; 11, gas analyzer; 12, signal booster; 13, multiplier.

comparison of design and experimental values of non-stationary pressure in the engine cylinder. First of all, it was necessary to find out whether the used variant k–ε – turbulence models (2) in a combination with combustion model (4) of Magnussen–Hjertager answers the real conditions in the gas-engine cylinder. Thus, it is necessary to mean that values of empirical factors B and C of combustion model (4) depend also on the accepted turbulence model and as it has been noted, there is a necessity of their experimental test. In Fig. 3, the example of calculation of non-stationary pressure in the cylinder is resulted at factor value $B = 23.3$, leading to the best coordination of experimental and design display diagrams (the deviation for a cycle maximum pressure makes 1.7%). For partial loading mode another value of this factor – $B = 17.7$ is established that it is possible to explain by means of the change of air excess factor λ (Figs. 3 and 4). Other empirical factor value from (4) was accepted as $C = 0.5 = \text{const}$.

The maximum deviation between design and experimental (i.e. calculated from the experimental display diagrams) values of speeds of heat generation in the cylinder does not exceed 6% (Fig. 4).

Further in calculations empirical factors values leading to the best coordination of experimental and design display diagrams were applied.

6. The analysis of numerical experiments results

The developed mathematical model allows carrying out numerical experiments in a wide range of constructive and adjusting parameters change. In this case the purpose of numerical experiments was to define optimum values of rotational charge motion intensity and ignition point of a gas mixture providing nitric oxides impoverishment in combustion materials of a gas engine.

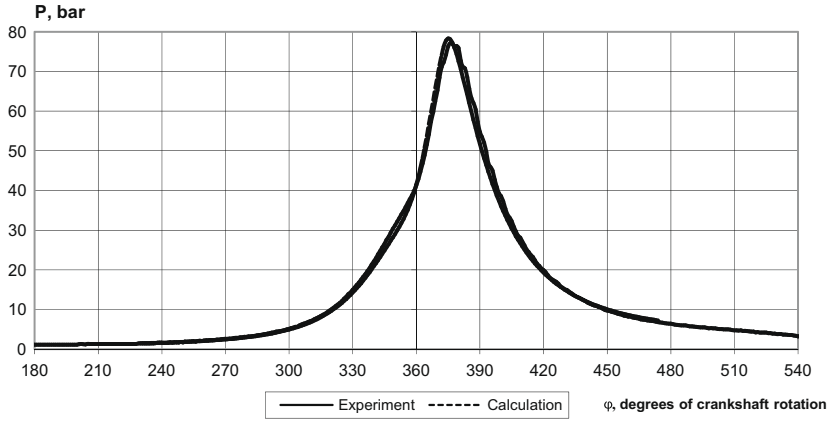

Fig. 3. Experimental and design changes of pressure in the gas-engine cylinder depending on a rotational angle of crankshaft (degrees of crankshaft rotation) on maximum capacity mode ($N_e = 176$ kW; $n = 2200$ min^{-1}, $\lambda = 1.3$).

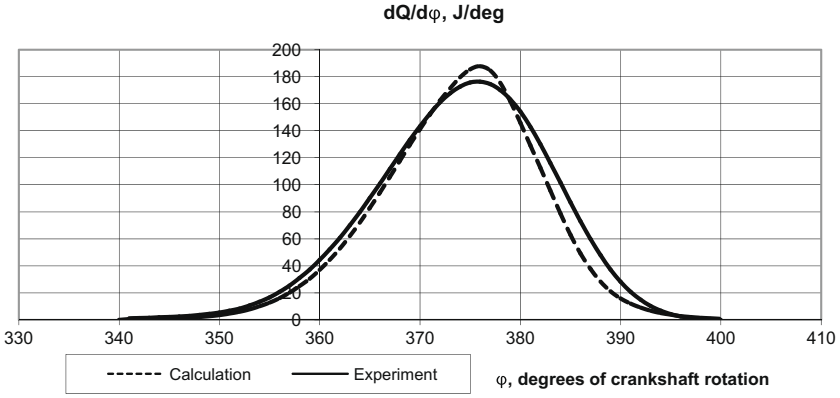

Fig. 4. Experimental and design rate of a heat generation in the gas-engine cylinder (a mode of partial loading $N_e = 156$ kW; $n = 1550$ min^{-1}, $\lambda = 1.5$).

6.1. Influence of rotational charge motion intensity on integrated and local parameters of working process

Rotational charge motion intensity at the moment of injection, and also at the moment of ignition of liquid (diesel) fuel as it was noted above, makes considerable impact on ecological and effective diesel engine factors [1,2]. The item is especially urgent regarding a diesel engine converted into a gas engine as modern high-speed diesel engines, as a rule, are equipped with the tangential and spiral inlet channels [2] established to generate rotational charge motion which intensity should correspond to a spray jet design, to fuel-supply parameters and fuel stream dynamics. In this connection, the question – how much the inlet channel of a serial diesel engine and rotational charge motion intensity, generated by this channel, correspond to the working process requirements of the engine converted into gas, – is urgent for modern engine-building.

In the present work as it is accepted in the theory of piston engines [2], rotational charge motion intensity in the cylinder, is estimated by the so-called vortical number $D_n = \frac{n_r}{n}$, where n_r is a rotary speed of the charge (in this case natural gas and air mixtures), rotating round a cylinder shaft practically under the law of rotation of a solid, n – a rotary speed of the engine crankshaft. Other rotational charge motion intensity indexes, used also at diesel engine working process development, can be received from the specified vortical number by simple recalculation [1].

Modeling of gas-engine working process was done for three various vortical number values $D_n = 0, 1$ and 2. It is obvious that the value $D_n = 0$ corresponds to an extreme case when the inlet channel does not generate rotational charge motion and the speed field in the cylinder is completely defined by piston motion. In Fig. 5, speed fields in one of the horizontal sections of the engine cylinder located at 2 mm distance from a cylinder cover surface (at level of spark plug electrodes) are resulted.

The intensity of air–gas mixture rotary motion in the end of the compression process essentially influences turbulence kinetic energy, combustion speed and a non-stationary temperature field of a working body in the chamber. For the considered variant of the chamber the process of compression without preliminary flux motion (i.e. in case of $D_n = 0$) is characterized by the highest turbulence kinetic energy. At the same time in most zones of the combustion chamber local values of this energy does not have a great difference and are close to size $k \approx 6$ m^2/s^2, time in a zone of the combustion chamber edge its maximum size reaches value $k \approx 17$ m^2/s^2.

In case of $D_n = 2$, the values make approximately $k \approx 4.5$ m^2/s^2 on total combustion chamber volume. The reason of kinetic energy decrease is the squish in super-piston volume [2,4] which is more obviously shown in the chamber with zero vortical number. During the moment $\phi = 360^\circ$ of piston top dead point reaching the average value of k on the total volume for variants with vortical numbers 1 and 2, is almost identical. Turbulent speed pulsations in the spacing between the piston and a head are blanked out, and turbulence kinetic energy takes minimum values. However such kind of

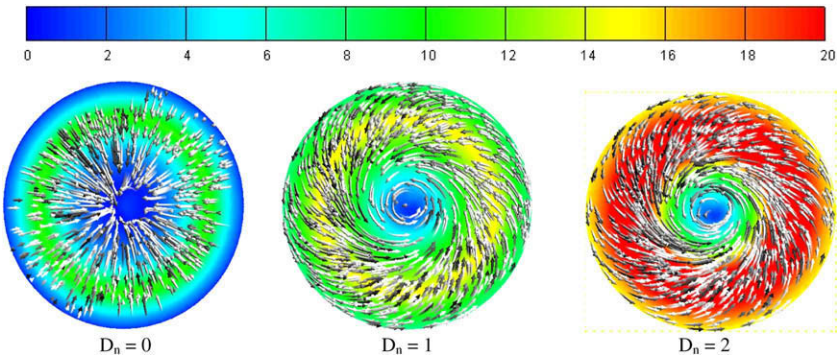

Fig. 5. Speed fields of a charge in the gas-engine cylinder with the symmetric combustion chamber depending on rotational motion intensity ($\phi = 345^\circ$, a mode of partial loading $N_e = 156$ kW; $n = 1550$ min^{-1}, the section location – 2 mm from a cylinder cover surface, at level of spark plug electrodes).

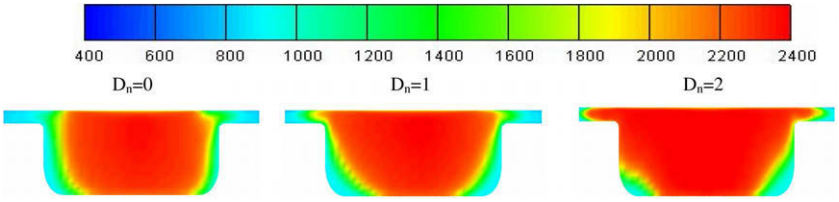

Fig. 6. Local temperatures of working body (K) in the gas-engine cylinder with a symmetric combustion chamber depending on rotational charge motion intensity ($\phi = 375^\circ$, a mode of partial loading $N_e = 156$ kW; $n = 1550$ min^{-1}).

k – fields instantly starts to be broken, as soon as expansion starts and the piston begins to move to low dead point.

In case of working body rotation absence ($D_n = 0$), the local temperatures in the chamber are distributed in such a way (Fig. 6) that in wall zones, especially in a spacing between the piston and the cylinder head, near the wall and in zones of the chamber bottom roundings, "cold" areas are formed. There is enough of low-temperature working body promoting the formation of unburnt hydrocarbons HC which exhaust in atmosphere are limited by legislative rules. From this point of view increase of rotational charge motion intensity to $D_n = 2$ (Fig. 6) leads to the best hot combustion materials mixing with a fresh charge, to reduction of cold wall zones, more equal temperature distribution on volume, and as a result, to HC impoverishment.

The increase in vortical number to $D_n = 2$ leads to increase in speed of combustion and a cycle maximum pressure p_z, at the same time temporal shift p_z in comparison with $D_n = 0$ can reach 7° a crankshaft angle that is considerably reflected in a display engine power. The change of the averaged in volume temperature of a working body in the cylinder (Fig. 7) has the similar character, at that if a difference between the maximum values of temperatures T_z for $D_n = 0$ and $D_n = 1$ makes all ~20 K for $D_n = 1$ and $D_n = 2$ it already reaches ~100 K.

The local values of nitric oxides concentration in a combustion process (Fig. 8) are caused by local temperatures values, and also local factors of air excess. As shown in Fig. 8, in 56° crankshaft angle (on the given mode it corresponds to ~6 ms) after the combustion commencement, the area of formed NO_x for a variant with vortical number 2, almost in 5 times more than for other investi-

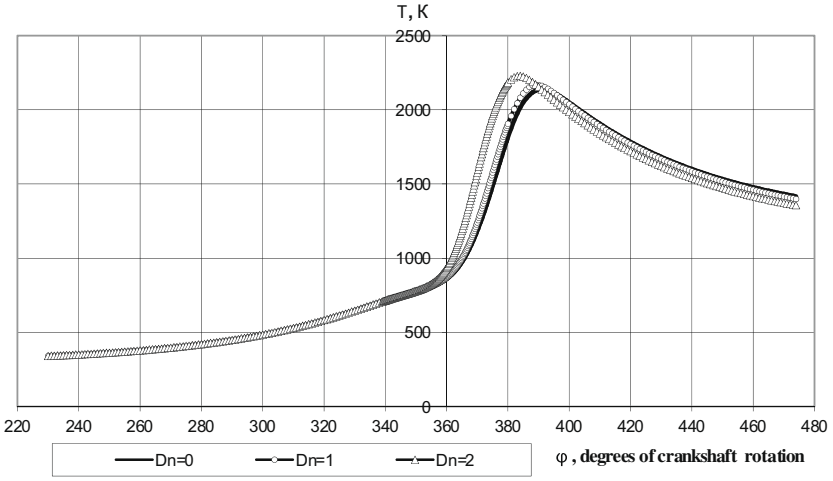

Fig. 7. Averaged in volume non-stationary temperature of the working body in the gas-engine cylinder with a symmetric combustion chamber depending on rotational charge motion intensity (a mode of partial loading $N_e = 156$ kW; $n = 1550$ min^{-1}).

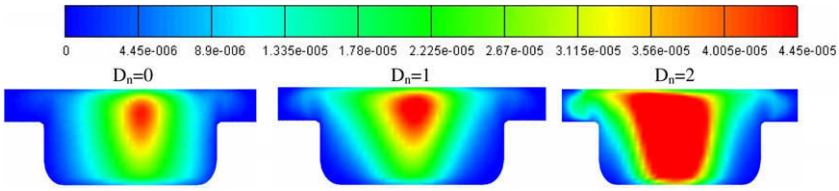

Fig. 8. Local values of NO_x concentration in the gas-engine cylinder with the symmetric combustion chamber depending on rotational charge motion intensity ($\phi = 390^\circ$, a mode of partial loading $N_e = 156$ kW; $n = 1550$ min^{-1}).

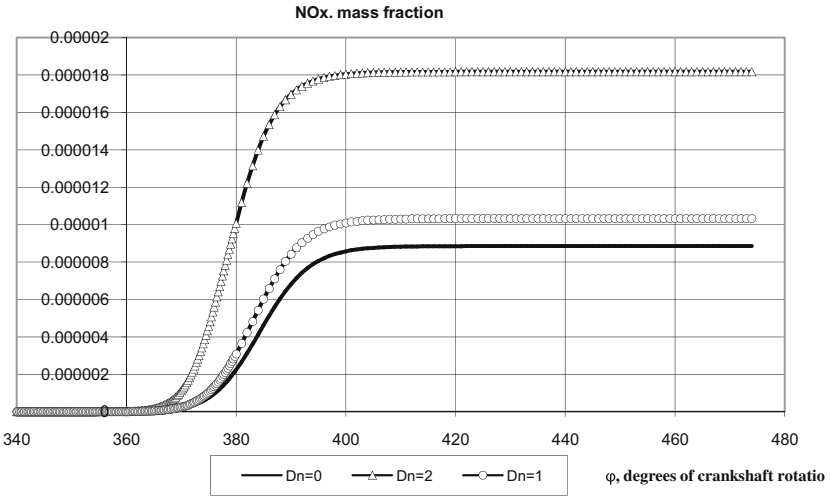

Fig. 9. Total concentration formed for a work nitric oxides cycle in the gas-engine cylinder with a symmetric combustion chamber depending on rotational charge motion intensity (a mode of partial loading $N_e = 156$ kW; $n = 1550$ min^{-1}).

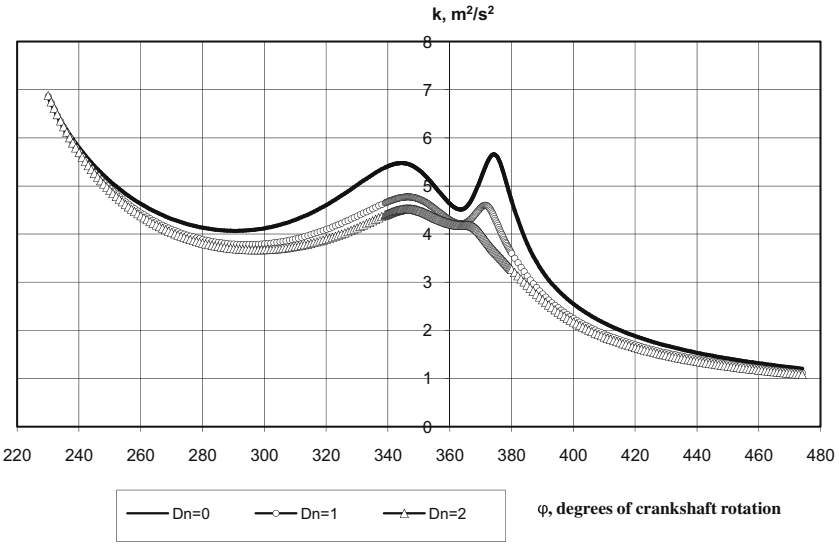

Fig. 10. The averaged turbulence kinetic energy in the gas-engine cylinder with the symmetric combustion chamber depending on rotational charge motion intensity (a mode of partial loading $N_e = 156$ kW; $n = 1550$ min^{-1}).

gated cases. It also proves to be true by the schedule of the averaged on total volume of the cylinder concentration NO_x change (Fig. 9).

It is necessary to notice that the turbulence kinetic energy change depending on rotational charge motion intensity in comparison with nitric oxides concentration change has an opposite character (Fig. 10). Thus in a combustion process, especially at small preliminary charge motion intensities, the change schedule of k has two strongly marked maxima – before top dead point $k_{\max 1}$ and after top dead point $k_{\max 2}$. Their values at $D_n = 0$ make $k_{\max 1} = 5.5$ and $k_{\max 2} = 5.7$ m^2/s^2, and for a variant with vortical number 2 decrease to $k_{\max 1} \approx 4.5$ and $k_{\max 2} = 4.2$ m^2/s^2 accordingly. It is also noticeable that with decrease of vortical number D_n kinetic energy of turbulence after top dead point becomes much smaller, than before top dead point. We will underline that at the maximum loading mode such strongly marked maxima are not observed.

The moment of spark ignition, i.e. the spark angle (θ), is an adjusting parameter and its value makes essential impact on effective and ecological indicators of the gas engine. It is obvious that available rotational charge motion intensity at the end of compression process should be coordinated with a spark angle. Numerical modeling of the working process has been carried out at various spark angles $\theta(-5^\circ, -10^\circ, -13^\circ, -15^\circ, -21^\circ, -25^\circ, -30^\circ, -35^\circ$ before top dead point). It is obvious that with the ignition delay (i.e. with approach of a angle of the ignition beginning to TDP) the maximum pressure p_z in the cylinder decreases and comes later. Maximum pressure values, for example, at spark angles $\theta = -35^\circ$ and $\theta = -5^\circ$ differ essentially from each other almost twice, and phase shift between them makes 22°. Dependence on the averaged in cylinder volume temperature from θ has the similar but not so obvious character. In fact, for spark angles $-35°$, $-30°$, $-25°$, $-21°$ the temperature maximum makes approximately 2360 K, having only phase shift difference approximately at 1° a crankshaft angle. Further the difference is more obvious, and for $\theta = -5^\circ$ the temperature maximum decreases to 2024 K that is only at 15% less than for $\theta = -35^\circ, -30^\circ, -25^\circ, -21^\circ$ and reaches at approximately 28° crankshaft angle later. Spark angle has considerable influence on NO_x formation dynamics in the combustion chamber. It is obvious that NO_x concentration decreases approximately at 28% with the approach of the spark angle to top dead point that, first of all, is explained by the temperature decrease, and the quantity of NO_x formed at $\theta = -5^\circ$ makes only 3.6% from the quantity of nitric oxides, exhausted at $\theta = -35^\circ$. It is possible to conclude that an spark angle as an adjusting parameter of the working process should be optimized at carrying out of any of the actions considered above and directed to nitric oxides impoverishment in the gas-engine exhausts.

7. Conclusion

Lower cost of natural gas and its large supplies in comparison with liquid hydrocarbonic fuels make the gas engine preferable in comparison with the engines working on traditional liquid fuels. The advantage of the diesel engines converted into the gas engine with spark ignition, in comparison with the diesel engines converted into gas–liquid engine, is, first of all, in the absence of firm particles of soot of a fuel origin in combustion products. In the given work the concept of the gas engine working on impoverished mixes ($\lambda \geqslant 1.3$) has been chosen.

On the basis of the fundamental equations of movement quantity, energy, concentration and weight transport, and also chemical kinetics in common with the turbulence models, it is more convenient to realize with the application of the program complex FIRE, focused on the solution of piston engines problems and, allowing to use moving boundaries of a calculating area. Model application of Magnussen–Hjertager for calculation of turbulent combustion in gas engines, and also Zeldovich's expanded thermal mechanism – for calculation of nitric oxides concentration, give the results, having a good consistency with experimental data.

The analysis of the influence of the rotational charge motion intensity on the engine working process has shown that the increase in vortical number D_n leads to increase in the maximum values of pressure and temperatures in the cylinder. So, working with $D_n = 2$, p_z is higher than in all other investigated cases at 20%. However, the quantity of NO_x formed in this case is also maximum and surpasses other variants approximately in 2 times. Hence, it is possible to draw a conclusion that to obtain good effective engine indicators, it is necessary to use system with the maximum rotational motion intensity of air–fuel mixture. And on the contrary, obtain good ecological indicators, it is expedient to use the inlet system leading to a less stream motion (spin).

As a result of the researches the conclusion that converting of a diesel engine of KamAz-740.13-240 into a natural gas one with spark ignition is expedient, both from economic, and from the ecological point of view proves to be true. For the gas engine the spark angle $\theta = 26^\circ$ before top dead point for a rated power mode and $\theta = 21^\circ$ before top dead point for a partial loading mode (80% from rated power) is recommended; vortical number $D_n = 1$ for both modes, and the symmetric (cylindrical) form of the combustion chamber.

References

[1] G. Woshni, K. Zeilinger, R.Z. Kavtaradze, Air rotational motion in a high-speed diesel engine with four valves on the cylinder, Herald of the BMSTU (Bauman Moscow State Technical University) (1) (1997) 74–84.

[2] R. Van Basshuysen, F. Schäfer, Handbuch Verbrennungsmotor. Grundlage, Komponenten, Systeme, Perspektive. 4. Auflage, Vieweg & Sohn Verlag, Wiesbaden, 2007.

[3] R.Z. Kavtaradze, A.I. Gaivoronskii, V.A. Fedorov, D.O. Onishchenko, A.V. Shibanov, Calculation of radiative–convective heat exchange in the combustion chamber of a diesel engines, High Temp. 45 (5) (2007) 673–680.

[4] R.Z. Kavtaradze, Local Heat Exchange in Piston Engines, second ed., BMSTU (Bauman Moscow State Technical University), Moscow, 2007, 472 p.

[5] D. Andersen, G. Tannehil, R. Pletcher, Computing Hydromechanics and Heat Exchange (in two volumes), Moscow, "Mir", vo1. 1, 1990, 384 p, vol. 2, 1990, 392 p.

[6] D. Byun, S.W. Baek, Numerical investigation of combustion with non-gray thermal radiation and soot formation effect in a liquid rocket engine, Int. J. Heat Mass Transfer 50 (3–4) (2007) 412–422.

[7] U.A. Bystrov, S.A. Isaev, N.A. Kudryavtsev, A.I. Leontiev, Numerical Modeling of a Vortical Intensification of Heat Exchange in Packages of Pipes, Sudostroenie, St. Petersburg, 2005.

[8] D.B. Spalding, Combustion and Mass Transfer, Pergamon Press, Oxford, New York, Toronto, Sydney, Paris, Frankfurt, 1985.

[9] B.F. Magnussen, B.H. Hjertager, On mathematical modelling of turbulent combustion with special emphasis on soot formation and combustion, in: 16th Symposium (Int) on Combustion, The Combustion Institute, 1976.

[10] G. Merker, Ch. Schwarz, G. Stiesch, F. Otto, Verbrennungsmotoren Simulation der Verbrennubg und Schadstoffbildung. 3. Auflage, Teubner-Verlag Stuuugart, Leipzig, Wiesbaden, 2006.

[11] F. Chmela, D. Dimitrov, G. Pirker, A. Wimmer, Konsistente Methodik Vorausrechnung der Verbrennung in Kolbenkraftmaschinen, MTZ (6) (2006) S.468–S.475.

[12] N.A. Ivashchenko, R.Z. Kavtaradze, A.S. Golosov, Z.R. Kavtaradze, A.A. Skripnik, Method of calculation of local concentration of nitric oxides in piston engines with internal carburetion on a basis multizone models, Herald of the BMSTU (Bauman Moscow State Technical University) (1) (2004) 43–59.

[13] S.M. Frolov, A.A. Skripnik, R.Z. Kavtaradze, Modelling of Diesel Spray Ignition Semenov Memorial. Combustion and Atmospheric Pollution, Torus Press Ltd., Moscow, 2003.

[14] S.M. Frolov, A.A. Skripnik, R.Z. Kavtaradze, V.V. Efros, Ignition modelling in liquid fuel stream, Chem. Phys. 23 (1) (2004) 54–61.

[15] FIRE, Users Manual Version 8.5. AVL List GmbH Graz, Austria, 2007 (licence agreement DKNR: BMSTU 101107 between BMSTU (Bauman Moscow State Technical University) and "APS Consulting").

[16] S. Patankar, Numerical Methods of the Solution of Heat Exchange Problems and of Dynamics of a Liquid, Energoatomizdat, Moscow, 1984. 152 p.

[17] G. Hyun, D. Lee, Sh. Goto, KIVA simulation for mixture formation processes in an in-cylinder-injected LPG SI engine SAE Paper, Baltimore, No. 12001-01-2805, 2000.